

A user-friendly package and workflow for generating effective homogeneous rheologies for the study of the long-term orbital evolution of multilayered planetary bodies

Yeva Gevorgyan¹

King Abdullah University of Science and Technology (KAUST), Thuwal, Saudi Arabia
e-mail: yeva.gevorgyan@kaust.edu.sa

Received March 17, 2026; accepted XXX

ABSTRACT

Context. Tidal dissipation plays an important role in the long-term orbital evolution of planets and moons. For stratified viscoelastic bodies, evaluating the frequency-dependent tidal response during long-term dynamical integrations is computationally expensive, since it requires repeatedly solving the internal deformation problem. Therefore, orbital evolution codes benefit from effective homogeneous rheologies that approximate the dissipation of stratified interiors at low computational cost.

Aims. We present a user-friendly, open-source Wolfram Language package that automates the construction of an effective homogeneous generalized Voigt rheology for a spherically symmetric, incompressible layered body with Maxwell solid layers. It provides a practical bridge between layered interior models and time-domain simulations of tidal evolution.

Methods. The package combines three components: (i) a forward computation of the degree-2 tidal Love number based on the propagator-matrix formulation for incompressible stratified viscoelastic bodies; (ii) numerical identification of the secular relaxation poles and residues of the layered model; and (iii) inversion of the resulting response into the compliance of an equivalent homogeneous generalized Voigt body. The implementation is based on the equivalence established for multilayer Maxwell bodies and includes an optional dominant-mode selection procedure for obtaining reduced rheological models over a prescribed frequency range.

Results. The package returns the parameters of the equivalent homogeneous model, including elastic, gravitational, viscous, and Voigt-element contributions, in a format suitable for downstream numerical applications. As a case study, we apply the package to a five-layer lunar interior model and obtain its equivalent generalized Voigt representation, together with a reduced model that preserves the tidal response over the frequency interval relevant for orbital evolution while using fewer relaxation elements.

Conclusions. This package makes the reduction from stratified viscoelastic interiors to effective homogeneous rheologies reproducible and accessible. It allows physical tidal dissipation models to be used in long-term orbital and spin-evolution studies without having to repeatedly solve the full layered boundary-value problem.

Key words. planets and satellites: interiors – planets and satellites: dynamical evolution and stability – methods: numerical

1. Introduction

Tidal deformation and energy dissipation play an important role in the long-term orbital evolution of planets and moons. The magnitude and frequency of tidal dissipation depend on the internal structure of the deformable body, in particular on the distribution of density, elasticity, and viscosity.

Tidal deformation is modeled with the frequency-dependent degree-2 tidal Love number $k_2(s)$, that can be obtained by solving the governing equations for a radially stratified viscoelastic body. Here, the stratified forward model follows the propagator-matrix formulation for incompressible, spherically symmetric stratified bodies in Sabadini et al. (2016, Chapter 2). Solid layers are modeled with Maxwell rheology, and liquid layers through the appropriate small-shear limit. This approach is a consistent way to evaluate the tidal response of the body, but can become too costly to solve repeatedly within long-term orbital or spin-evolution integrations.

Long-term dynamical evolution codes often rely on simplified homogeneous rheologies or empirical prescriptions, such as constant time lag, constant phase lag, or single-element Maxwell models. These approximations are computationally convenient, but generally fail to reproduce the multiple relaxation timescales

and dissipation peaks that arise in layered bodies Gevorgyan (2021); Bolmont et al. (2020). In Gevorgyan et al. (2023), the authors showed that, under the assumptions of a simple multilayer rheology, the tidal response of a stratified body can be modeled by a homogeneous body with a sufficiently complex generalized rheology, like a generalized Voigt model. This prompted us to develop a relatively simple workflow that allows one to replace the stratified problem with an effective homogeneous model without losing the frequency-dependent tidal response.

In this work we present an open-source Wolfram Language package¹ that takes a user-specified multi-layered model and constructs the corresponding effective homogeneous generalized Voigt rheology. The input file contains the layer radii, densities, shear moduli, viscosities, and forcing frequency, and the main routine performs the full reduction pipeline: computation of $k_2(s)$ for the layered model, identification of secular poles and residues, inversion to the equivalent compliance function, and extraction of the generalized Voigt parameters. An optional reduction step identifies dominant relaxation modes over a user-defined frequency interval, yielding a compact model when an exact full representation is unnecessary.

¹ <https://github.com/ygevorgyan/HomogeneousModel>

Our implementation was partly motivated by the need to connect detailed geophysical interior models with modern time-domain orbital integrators such as the *RheoVolution* (de Oliveira et al. 2025a,b), which can evolve deformable bodies with complex homogeneous rheologies but require as input the parameters of an effective rheological model rather than a full multilayer interior description. Our package fills this gap by translating a stratified viscoelastic body into a homogeneous generalized Voigt one directly usable in such simulations.

The paper is organized as follows. In Section 2, we summarize the theoretical framework for the effective homogeneous rheology and its relation to the layered tidal response. In Section 3, we describe the structure of the software package, its inputs and outputs, and the computational workflow. In Section 4, we illustrate the method with an application to a five-layer model of the Moon and show how the package recovers the equivalent generalized Voigt rheology and, if desired, an optional reduced model that captures the tidal response over the frequency interval of interest. In Section 5 we conclude the paper with observations on the purpose and scope of the work and a few perspectives for improvement.

2. Theoretical background

This section summarizes the theoretical elements relevant to the software pipeline. The forward computation of the layered tidal response follows the propagator-matrix formulation for incompressible, stratified viscoelastic bodies presented in Sabadini et al. (2016), while the reduction to an equivalent homogeneous rheology is based on Gevorgyan et al. (2023).

2.1. Layered viscoelastic model

Consider a spherically symmetric body of N incompressible, homogeneous layers, each with outer radius r_k , density ρ_k , rigidity μ_k , and viscosity η_k . Solid layers are assumed to have Maxwell rheology, and their complex shear modulus in the Laplace domain is

$$\hat{\mu}_k(s) = \frac{\mu_k \eta_k s}{\mu_k + \eta_k s}. \quad (1)$$

The tidal response is described by the degree-2 Love number $k_2(s)$, obtained from the propagator-matrix solution of the governing equations for a stratified body. All layers are treated within a unified propagator formulation, and liquid layers are handled in the small-shear limit, see Subsection 3.3.

For a finite multilayer Maxwell body, $k_2(s)$ is a rational function of the Laplace variable and admits the mode decomposition

$$k_2(s) = k_E + \sum_{i=1}^n \frac{r_i}{s - s_i}, \quad (2)$$

where k_E is the elastic Love number, $s_i < 0$ are the secular poles, r_i are the corresponding residues, and $\tau_i = -s_i^{-1}$ are the relaxation times. Thus, the layered tidal response is fully characterized by the set of parameters $\{k_E, s_i, r_i\}$.

2.2. The homogeneous model

The equivalent homogeneous representation of stratified bodies is given by a generalized Voigt rheology in Figure 1. The Love number of the body is (Gevorgyan et al. 2023)

$$k_2(s) = \frac{3I_o G}{R^5} C(s), \quad (3)$$

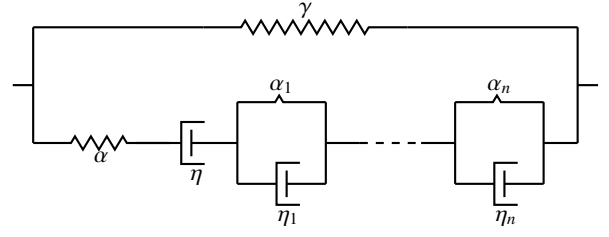


Fig. 1: Schematic representation of the generalized Voigt model.

where I_o is the mean moment of inertia, $C(s)$ is the complex compliance, and R is the mean radius of the body. The gravitational rigidity γ is defined from the fluid Love number k_f as (Correia et al. 2018)

$$\gamma = \frac{3I_o G}{R^5} \frac{1}{k_f}. \quad (4)$$

For the generalized Voigt rheology, the complex compliance is decomposed as

$$C(s) = \frac{1}{\alpha + \gamma} + C_v(s), \quad (5)$$

where α is the elastic rigidity and $C_v(s)$ contains the viscous contribution of the dashpot and a finite number of Kelvin–Voigt elements in Figure 1. The equivalent homogeneous model is specified by the parameters $\{\gamma, \alpha, \eta, \alpha_i, \eta_i\}$.

2.3. Connection with the software workflow

The software automates the passage from the layered model to the homogeneous one in three steps. First, it computes the layered Love number $k_2(s)$ (the tidal Love number computed for the layered interior model) from the propagator formulation. Second, it identifies the secular poles s_i and residues r_i in the decomposition (2). Third, it constructs the compliance $C(s)$ from equations (3)–(5) and extracts the parameters of the equivalent generalized Voigt model.

The explicit use of the pole–residue representation of the layered Love number as the intermediate object in the inversion pipeline is particularly effective from both a numerical and conceptual standpoint. It provides a compact spectral description of the viscoelastic response that is well suited to numerical computation and allows the equivalent generalized Voigt rheology to be constructed in a physically interpretable way.

3. Software implementation and workflow

The package is written in Wolfram Language as a modular pipeline for constructing the homogeneous generalized Voigt rheology of a layered viscoelastic body. The model is not hard-coded to any specific planetary interior: all physical and numerical inputs are supplied by the user through a configuration file, and the same workflow applies to any incompressible, spherically symmetric multilayer model satisfying the assumptions discussed in Section 2.

3.1. Package structure

The code is organized into a small set of modules with distinct roles. The file `ModelInput.wl` contains the user-

specified physical model and numerical settings. The core routines are called by `computeHomogeneous`, implemented in `HomogeneousRheology.wl`, which evaluates the layered tidal response, extracts the secular poles and residues, and returns the parameters of the equivalent generalized Voigt model. A driver script, `RunHomogeneous.wl`, loads the modules, executes the full pipeline, prints summary tables, and generates comparison plots. A separate script, `VisualizeLayers.wl`, produces a cross-sectional visualization of the layered body directly from the same input file.

3.2. Input configuration

The file `ModelInput.wl` contains both the physical description of the layered body and a small set of numerical controls for the inversion pipeline. The same workflow can be applied to any spherically symmetric multilayer configuration once the corresponding layer properties and forcing frequency are provided.

The physical model is specified through the arrays of outer radii, densities, rigidities, and viscosities of the layers, together with the tidal forcing frequency. An optional list of layer names may be supplied for visualization purposes. All physical quantities are given in SI units, and all arrays must have the same length, which determines the number of layers in the model. Liquid layers are identified through the condition $0 < \mu < 1$ Pa; for such layers, the method uses an effective elasticity value to regularize the small-shear limit (Sabadini et al. 2016).

The same input file contains numerical settings that control the precision of the calculations, the search interval used to detect the secular poles, and the frequency range and threshold adopted in the dominant-mode selection step. These parameters are not part of the planetary model but determine how the software resolves the relaxation spectrum and how aggressively the final generalized Voigt model is reduced. Their default values are listed in Table 1.

3.3. Main routine and computational workflow

The main routine

```
computeHomogeneous[rk, rhok, muk, etak, omega, opts]
```

performs the parameter extraction through the sequence of operations illustrated in Fig. 2. It follows the same three-step structure of Sections 1 and 2: forward computation of the layered Love number, mode decomposition, and rheological inversion. The code first evaluates the elastic Love number k_E and the complex tidal response $k_2(i\omega)$ for the layered body. It then searches for the zeros of the secular determinant on the negative real axis, refines them numerically, and computes the corresponding residues. From these quantities it evaluates the fluid Love number k_f , the mapping constants Θ , γ , and α , and finally constructs the compliance

$$C(s) = \frac{k_2(s)}{\Theta - \gamma k_2(s)}, \quad (6)$$

from which the parameters $\{\eta, \alpha_i, \eta_i\}$ of the Voigt model are extracted.

The forward layered problem is evaluated through a unified 6×6 propagator matrix approach for all layers. Liquid layers are treated by small-shear regularization, such that solid and liquid regions are handled within the same numerical framework. This is an important practical point: the current package does

Table 1: Main user inputs and numerical controls of the Wolfram package. Physical quantities are supplied through `ModelInput.wl`; optional numerical settings control pole search and dominant-mode selection.

Key	Units/default	Description
<i>Physical model</i> (<code>\$ModelConfig</code>)		
<code>rk</code>	m	Layers' outer radii
<code>rhok</code>	kg m ⁻³	Layers density
<code>muk</code>	Pa	Layers' shear moduli
<code>etak</code>	Pa s	Layers' viscosities
<code>omega</code>	rad s ⁻¹	Tidal forcing frequency
<code>layerNames</code>	optional	Optional list of layer labels
<i>Numerical settings</i> (<code>\$AnalysisConfig</code>)		
<code>workingPrecision</code>	50	Numerical working precision in digits
<code>gridLogMin</code>	-20	Lower bound of the pole-search interval in log ₁₀ s
<code>gridLogMax</code>	-3	Upper bound of the pole-search interval in log ₁₀ s
<code>gridPoints</code>	2000	Number of grid points used to detect sign changes in the secular determinant
<code>omegaInterestMin</code>	10 ⁻¹⁰ rad s ⁻¹	Lower bound of the frequency interval used for dominant-mode selection
<code>omegaInterestMax</code>	10 ⁻⁵ rad s ⁻¹	Upper bound of the frequency interval used for dominant-mode selection
<code>dominantThreshold</code>	1/50	Fractional contribution threshold used to retain dominant Voigt elements

not switch to a separate Clairaut propagator for liquids, but instead uses a single propagation formalism for arbitrary combinations of solid and liquid layers. A true liquid has $\mu = 0$, but the Y -matrix (Sabadini et al. 2016, Eq. 2.42) contains terms of the form μ/r in rows 3, 4, and 6. Setting $\mu = 0$ exactly would therefore make these rows degenerate, causing the linear solver to fail when computing the propagator

$$P(r_2, r_1) = Y(r_2)Y^{-1}(r_1). \quad (7)$$

Instead, we assign a very small effective rigidity $\hat{\mu} \approx 10^{-20}$ Pa to liquid layers. This keeps the matrix full-rank and invertible, while making the shear-stress rows effectively zero to machine precision. This value is negligible compared with physical shear moduli, which are typically of order 10^9 – 10^{11} Pa, but remains large enough to preserve numerical stability at all reasonable (actually, even at quite stringent) working precisions. This is a standard regularization in viscoelastic normal-mode calculations to avoid introducing a separate 2×2 or 4×4 propagator for liquid layers while yielding numerically identical results.

After the full generalized Voigt model is obtained, the package performs an optional dominant-mode reduction. For each Voigt element, it evaluates the maximum fractional contribution to $-\text{Im}[C(i\omega)]$ over a user-defined frequency interval $[\omega_{\min}, \omega_{\max}]$. Elements whose contribution exceeds the prescribed threshold are kept in the reduced model. This produces a compact, effective rheology targeted to the frequency interval most relevant for the intended dynamical application.

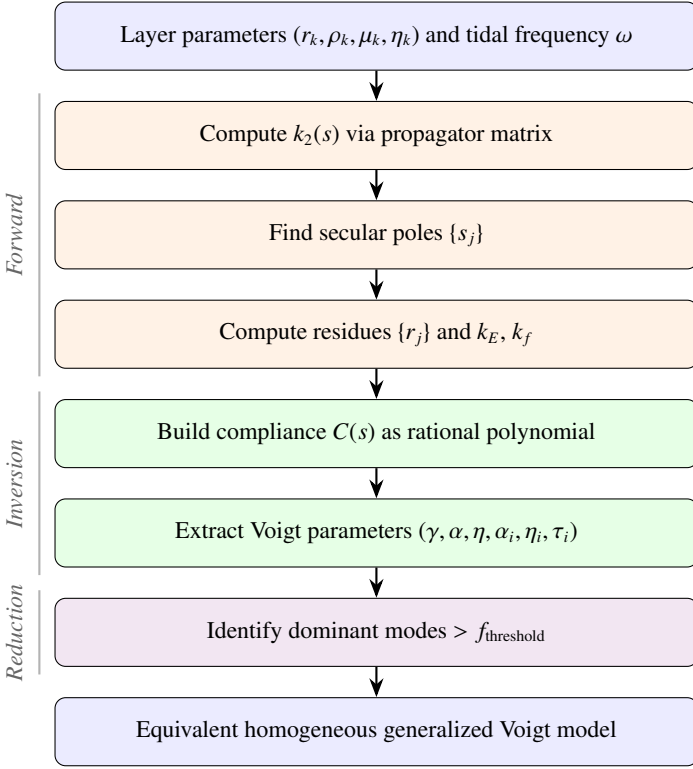


Fig. 2: Workflow of the computeHomogeneous pipeline.

3.4. Output

The main routine `computeHomogeneous` returns the layered response and its homogeneous representation as a Wolfram Association, and also exports the corresponding results to a JSON file. The package also returns the intermediate modes used in the inversion. In this way, the user has access both to the physical outputs of interest—the effective generalized Voigt parameters—and to the pole–residue decomposition that connects the layered model to the homogeneous model. The returned quantities are summarized in Table 2.

The output falls into three groups: the Love numbers of the layered body, the constants used in the layered-to-homogeneous mapping, and the relaxation modes and rheological parameters of the equivalent generalized Voigt model. This organization separates diagnostic quantities from the final effective model. The Love-number and mode outputs are used to check the inversion, and the generalized Voigt parameters are used in downstream applications. The package also generates summary tables, dominant-mode diagnostics, and comparison plots. The outputs can be used for both analysis and reuse. The user can inspect the mode decomposition, compare the full and reduced models, or export the reduced generalized Voigt parameters to an external integrator such as *RheoVolution* (de Oliveira et al. 2025a,b).

4. Case study: A five-layer model of the Moon

To test the package, we use the five-layer lunar model of Gevorgyan et al. (2023) to illustrate the equivalence between a multilayer Maxwell body and an effective homogeneous rheology. The model parameters are summarized in Table 3, and its cross-section is illustrated in Fig. 3; the figure was automatically produced by `VisualizeLayers.wl` module. The Moon

Table 2: Quantities returned by `computeHomogeneous`. The routine returns both the intermediate mode information of the layered model and the parameters of the equivalent homogeneous generalized Voigt rheology.

Key	Units	Description
kE	dimensionless	Elastic Love number k_E
kf	dimensionless	Fluid Love number k_f
k2Re	dimensionless	Real part of $k_2(i\omega)$
k2Im	dimensionless	Imaginary part of $k_2(i\omega)$
gamma	Pa	Gravitational rigidity γ
alpha	Pa	Elastic rigidity α
eta	Pa s	Viscosity of the isolated dashpot
prefactor	s^{-2}	Mapping prefactor $\Theta = 3I_0 G/R^5$
Fconv	$Pa s^2$	Conversion factor to physical units
nPoles	integer	Number of secular poles M
poles	s^{-1}	Secular pole locations $\{s_j\}$
residues	dimensionless	Residues $\{r_j\}$ in the mode decomposition of $k_2(s)$
nVoigt	integer	Number of Kelvin–Voigt elements N_V
tauV	s	Relaxation times $\{\tau_i\}$ of the Voigt elements
alphaV	Pa	Spring rigidities $\{\alpha_i\}$ of the Voigt elements
etaV	Pa s	Dashpot viscosities $\{\eta_i\}$ of the Voigt elements

is the default example configuration in the package. The package was also tested for Io, Europa, and Enceladus using models and data from Hussmann and Spohn (2004), Wahr et al. (2006), Bierson and Nimmo (2016), and Thomas et al. (2016), although we are only going to report the results for the Moon. The `ModelInput` file for these additional test cases can be found in the software package repository.

4.1. The homogeneous model

The software extracts the secular relaxation poles and residues listed in Table 4. These modes provide the normal-mode decomposition of the lunar tidal response and are used to construct the equivalent homogeneous rheology. The corresponding inversion yields the full equivalent generalized Voigt model, whose parameters are listed in Table 5 and 6.

In Figure 4 we compare the dissipative part $-\text{Im}[k_2(i\omega)]$, and the elastic part, $\text{Re}[k_2(i\omega)]$ of the layered moon model to the full homogeneous model. The agreement shows that the full equivalent

Table 3: Physical parameters for the 5-layer viscoelastic model of the lunar interior taken from Matsuyama et al. (2016, Table 2) and Gevorgyan et al. (2023).

Layer	r_k (km)	ρ_k (kg/m^3)	μ_k (GPa)	η_k (Pa·s)
1. Inner Core	213.52	7720.16	40	10^{21}
2. Outer Core	325.00	6700.00	10^{-10}	1
3. Lower Mantle	500.00	3800.00	60	5×10^{16}
4. Upper Mantle	1697.15	3356.00	62.5	10^{21}
5. Crust	1737.15	2735.00	15	10^{23}

Layered body — cross-section (visual thickness exaggerated)

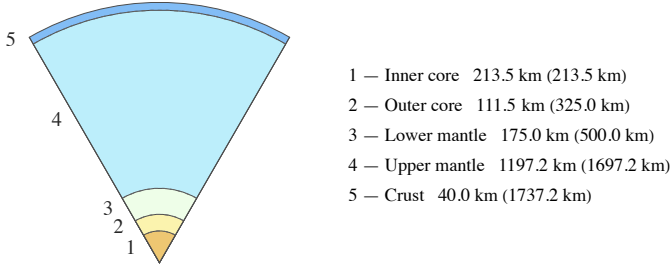


Fig. 3: Cross-section depiction of the 5-layer lunar interior model automatically generated by the `VisualizeLayers.wl` routine. The numbered list indicates the thickness of each corresponding layer, along with the position (radius) of its outer boundary in parentheses.

Table 4: Secular relaxation modes extracted for the 5-layer lunar model, sorted by relaxation timescale.

j	Pole s_j (s^{-1})	τ_j (s)	Residue r_j
1	-9.459×10^{-7}	1.057×10^6	8.098×10^{-10}
2	-6.342×10^{-7}	1.577×10^6	8.537×10^{-10}
3	-5.478×10^{-10}	1.826×10^9	1.922×10^{-14}
4	-1.709×10^{-12}	5.850×10^{11}	6.218×10^{-15}
5	-1.396×10^{-12}	7.165×10^{11}	1.563×10^{-12}
6	-1.230×10^{-13}	8.130×10^{12}	3.426×10^{-14}
7	-1.186×10^{-13}	8.434×10^{12}	4.908×10^{-16}
8	-2.446×10^{-14}	4.088×10^{13}	1.015×10^{-16}
9	-7.904×10^{-17}	1.265×10^{16}	4.080×10^{-20}

lent generalized Voigt model reproduces both the real and imaginary parts of the tidal Love number within numerical precision.

4.2. Dominant-mode reduction over a frequency interval

In many applications, it is unnecessary to retain the full effective rheology over the entire frequency range. The package includes a dominant-mode selection step that evaluates the maximum fractional contribution of each Voigt element to $-\text{Im}[C(i\omega)]$ over a prescribed interval of forcing frequencies and retains only those elements whose contribution exceeds a given chosen threshold.

For the Moon, the relevant frequency interval is $\omega \in [10^{-10}, 10^{-5}] \text{ rad s}^{-1}$ (the default package setting), and

Table 5: Extracted parameters for the Kelvin–Voigt elements of the full effective lunar model. Elements retained in the reduced model are marked with an asterisk.

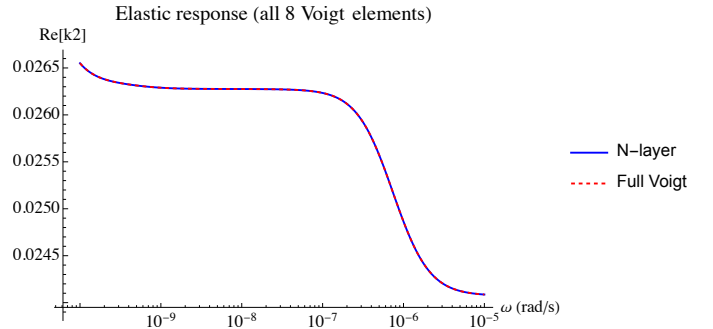
i	τ_i (s)	α_i (GPa)	η_i (Pa·s)
1*	4.230×10^{15}	8.273×10^{-4}	3.499×10^{21}
2	3.909×10^{13}	1.549×10^0	6.056×10^{22}
3	8.429×10^{12}	1.020×10^4	8.596×10^{25}
4*	2.623×10^{12}	5.530×10^{-1}	1.450×10^{21}
5	5.854×10^{11}	8.083×10^3	4.732×10^{24}
6	1.826×10^9	4.043×10^4	7.381×10^{22}
7*	1.578×10^6	1.048×10^3	1.654×10^{18}
8*	1.058×10^6	1.661×10^3	1.757×10^{18}

Table 6: Love numbers and effective rheological parameters for the lunar homogeneous model.

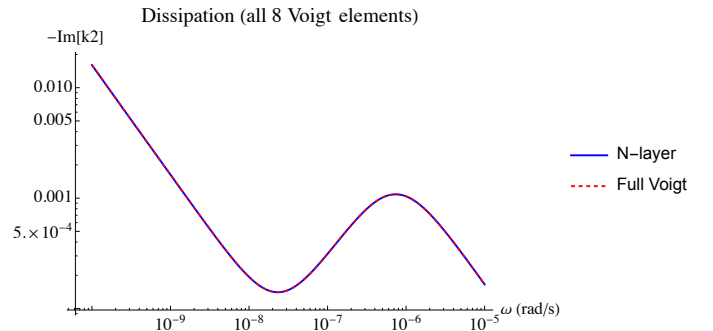
Quantity	Symbol	Value
Elastic Love number	k_E	2.40733×10^{-2}
Fluid Love number	k_f	1.43752
Real part of the Love number	$\text{Re}[k_2]$	2.42417×10^{-2}
Imaginary part of the Love number	$\text{Im}[k_2]$	-5.74359×10^{-4}
Gravitational rigidity	γ	1.020 GPa
Elastic rigidity	α	5.987×10^1 GPa
Dashpot viscosity	η	6.955×10^{21} Pa·s

we set the dominant-mode threshold to 2%. Under these assumptions, the full effective rheology is reduced to the subset of dominant Voigt elements marked with an asterisk in Table 5. As one can see from Fig. 4, the reduced model preserves the main features of the layered model in the selected frequency interval.

The reduction step is important from a practical perspective. It allows the user to tailor the effective homogeneous model to the frequency range relevant for a specific dynamical problem rather than to retain all relaxation modes of the exact inversion. The reduced model is therefore specific to the chosen frequency interval and dominant-mode threshold.



(a) Real part of the Love number, $\text{Re}[k_2(\omega)]$.



(b) Imaginary part of the Love number, $-\text{Im}[k_2(\omega)]$.

Fig. 4: Comparison between the exact five-layer lunar model and the equivalent homogeneous generalized Voigt model. The real and imaginary parts of the tidal Love number coincide within numerical precision when all extracted Voigt elements are retained.

5. Conclusions

We have presented a Wolfram Language package that automates the construction of effective homogeneous generalized Voigt rheologies for incompressible, spherically symmetric layered

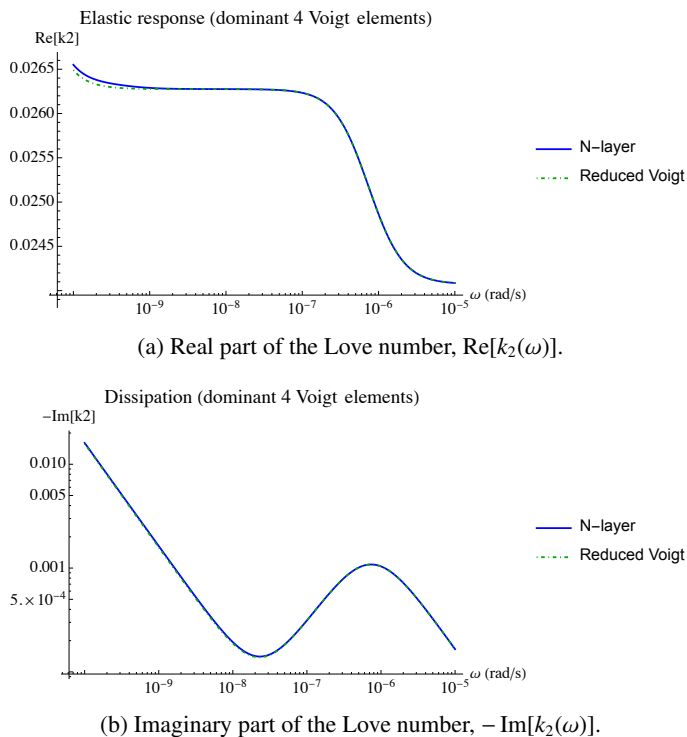


Fig. 5: Same as Fig. 4, but for the reduced equivalent homogeneous generalized Voigt model.

viscoelastic bodies. The package combines three components: the forward computation of the tidal Love number for a multilayer model, the numerical extraction of its secular poles and residues, and the inversion of the layered response into equivalent homogeneous rheology parameters. Starting from a user-defined layered model, the package returns the parameters of the corresponding homogeneous generalized Voigt body in a format suitable for validation, comparison, and downstream numerical use and applications.

The lunar case study illustrates the purpose of the software: to transform an interior model into a reproducible and computationally efficient homogeneous rheology. For a five-layer model including both solid and liquid regions, it recovers the equivalent homogeneous rheology together with a reduced model obtained through dominant-mode selection over a prescribed frequency interval. This reduction is particularly useful when the relevant forcing frequencies lie in a limited range, since it preserves the tidal response of the layered model while reducing the number of rheological elements.

The package allows detailed interior-structure models to be translated into generalized Voigt parameters that can be supplied directly to time-domain tidal evolution codes, enabling their dissipation properties to be incorporated in long-term orbital evolution calculations without repeatedly solving the full layered deformation problem during integration. We expect it to be useful for studies of the Moon, terrestrial planets, and icy satellites, especially in contexts where tidal dissipation must be coupled to orbital or rotational evolution over long timescales. Future developments may include extensions to broader classes of rheologies and tighter integration with external dynamical solvers.

Acknowledgements. The author would like to thank Clodoaldo Grotta Ragazzo (USP) for many discussions and long-standing collaboration on this topic, Diogo Aguiar Gomes (KAUST) for his kind support, and J. Ricardo G. Mendonça (USP) for technical advice and a careful reading of the manuscript that greatly

improved its presentation. This work was partially supported by the King Abdulah University of Science and Technology (KAUST), Saudi Arabia.

References

- R. Sabadini, B. Vermeersen, and G. Cambiotti. *Global Dynamics of the Earth*. Springer, 2016.
- Y. Gevorgyan. Homogeneous model for the TRAPPIST-1e planet with an icy layer. *A&A*, 650:A141, June 2021. .
- E. Bolmont, S. N. Breton, G. Tobie, C. Dumoulin, S. Mathis, and O. Grasset. Solid tidal friction in multi-layer planets: Application to Earth, Venus, a Super Earth and the TRAPPIST-1 planets. Potential approximation of a multi-layer planet as a homogeneous body. *A&A*, 644:A165, December 2020. .
- Y. Gevorgyan, I. Matsuyama, and C. Ragazzo. Equivalence between simple multilayered and homogeneous laboratory-based rheological models in planetary science. *MNRAS*, 523(2):1822–1831, August 2023. .
- V. M. de Oliveira, C. Ragazzo, and A. C. M. Correia. RheoEvolution: An N-body simulator for tidally evolving bodies with complex rheological models. *A&A*, 693:A5, January 2025a. .
- V. M. de Oliveira, C. Ragazzo, and A. C. M. Correia. RheoEvolution: Rheology evolution in the time domain. Astrophysics Source Code Library, record ascl:2508.007, August 2025b.
- A. C. M. Correia, C. Ragazzo, and L. S. Ruiz. The effects of deformation inertia (kinetic energy) in the orbital and spin evolution of close-in bodies. *Celestial Mechanics and Dynamical Astronomy*, 130(8):51, August 2018. .
- H. Hussmann and T. Spohn. Thermal-orbital evolution of Io and Europa. *Icarus*, 171(2):391–410, October 2004. .
- J. M. Wahr, M. T. Zuber, D. E. Smith, and J. I. Lunine. Tides on Europa, and the thickness of Europa’s icy shell. *Journal of Geophysical Research (Planets)*, 111(E12):E12005, December 2006. .
- C. J. Bierson and F. Nimmo. A test for Io’s magma ocean: Modeling tidal dissipation with a partially molten mantle. *Journal of Geophysical Research (Planets)*, 121(11):2211–2224, November 2016. .
- P. C. Thomas, R. Tajeddine, M. S. Tiscareno, J. A. Burns, J. Joseph, T. J. Lored, P. Helfenstein, and C. Porco. Enceladus’s measured physical libration requires a global subsurface ocean. *Icarus*, 264:37–47, Jan 2016. .
- I. Matsuyama, F. Nimmo, J. T. Keane, N. H. Chan, G. J. Taylor, M. A. Wieczorek, W. S. Kiefer, and J. G. Williams. GRAIL, LLR, and LOLA constraints on the interior structure of the Moon. *geophysical Research Letters*, 43(16):8365–8375, August 2016. .